



Published in final edited form as:

Cell Rep. 2021 August 03; 36(5): 109465. doi:10.1016/j.celrep.2021.109465.

## The residence of synaptically released dopamine on D2 autoreceptors

Alec F. Condon<sup>1</sup>, Brooks G. Robinson<sup>1</sup>, Naeem Asad<sup>2</sup>, Timothy M. Dore<sup>2</sup>, Lin Tian<sup>3</sup>, John T. Williams<sup>1,4,\*</sup>

<sup>1</sup>The Vollum Institute, Oregon Health Sciences University, Portland, OR, USA

<sup>2</sup>New York University Abu Dhabi, Saadiyat Island, P.O. Box 129188, Abu Dhabi, United Arab Emirates

<sup>3</sup>Department of Biochemistry and Molecular Medicine, School of Medicine, University of California, Davis, Davis, CA, USA

<sup>4</sup>Lead contact

### SUMMARY

Neuromodulation mediated by synaptically released endogenous transmitters acting in G-protein-coupled receptors (GPCRs) is slow primarily because of multistep downstream signaling. What is less well understood is the spatial and temporal kinetics of transmitter and receptor interaction. The present work uses the combination of the dopamine sensor, dLight, to detect the spatial release and diffusion of dopamine and a caged form of a D2-dopamine receptor antagonist, CyHQ-sulpiride, to rapidly block the D2 autoreceptors. Photoactivation of the CyHQ-sulpiride blocks receptors in milliseconds such that the time course of dopamine/receptor interaction is mapped onto the downstream signaling. The results show that highly localized release, but not dopamine diffusion, defines the time course of the functional interaction between dopamine and D2 autoreceptors, which determines downstream inhibition.

### Graphical Abstract

---

This is an open access article under the CC BY-NC-ND license (<http://creativecommons.org/licenses/by-nc-nd/4.0/>).

\*Correspondence: [williamj@ohsu.edu](mailto:williamj@ohsu.edu).

#### AUTHOR CONTRIBUTIONS

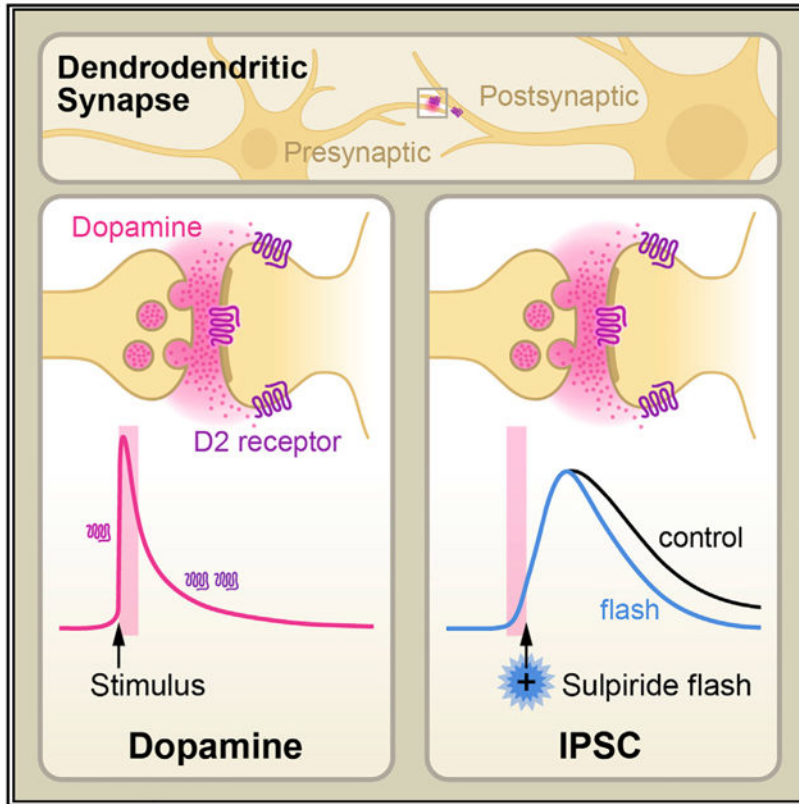
A.F.C., B.G.R., and J.T.W. designed and performed the experiments. L.T. provided the dLight1.3b and advice on the use and analysis of the imaging experiments. T.M.D. and N.A. provided the CyHQ-sulpiride. All authors contributed to the writing of the manuscript.

#### DECLARATION OF INTERESTS

The authors declare no competing interests.

#### SUPPLEMENTAL INFORMATION

Supplemental information can be found online at <https://doi.org/10.1016/j.celrep.2021.109465>.



### In brief

Somatodendritic release of dopamine via D2 autoreceptors activates an inhibitory postsynaptic current. The synaptic current is dependent on a transiently high concentration of dopamine. Condon et al. use a combination of optical and electrical approaches to show the spatial and temporal substrates of dendrodendritic transmission in the substantia nigra.

## INTRODUCTION

It has been known for decades that the activation of D2 autoreceptors with the exogenous application of agonists cause a potassium conductance-mediated inhibition of neurons in the substantia nigra and ventral tegmental area (Lacey et al., 1987). In more recent years, electrical stimulation has been used to evoke endogenous dopamine release to drive a D2-autoreceptor-dependent inhibitory postsynaptic current (IPSC, Beckstead et al., 2004). The lack of identifiable recurrent collaterals extending from dopamine neurons led to the conclusion that dopamine release in substantia nigra was from dendrites (Hajdu et al., 1973; Wilson et al., 1977; Groves and Linder 1983). The release of dendritic dopamine appears to be mechanistically similar to axonal release from projections in that it is calcium dependent, vesicular, exhibits spontaneous release, and is dependent on RIM, a key scaffolding protein linked to transmitter release (Gantz et al., 2013; Robinson et al., 2019). However, the lack of clearly identifiable anatomical sites of dendrodendritic transmission has created controversy

and limited the understanding of this from of endogenous modulation (Cragg and Rice 2004; Wiencke et al., 2020).

The present investigation addressed the spatial and temporal substrates of dendrodendritic transmission in the substantia nigra using the combination of the dopamine sensor, dLight (Patriarchi et al., 2018) and a photoactivatable D2 receptor antagonist, CyHQ-sulpiride (Asad et al., 2020). Imaging of dLight fluorescence following electrical stimulation found small isolated sites of intense fluorescence that followed stimulation. Photoactivation of CyHQ-sulpiride was used to rapidly block D2 autoreceptors (Asad et al., 2020). The timing of photoactivation relative to the electrical stimulation used to activate the IPSC was used to determine the time course of dopamine/D2-autoreceptor activation. The results show the peak amplitude of the IPSC was blocked or reduced by antagonism of D2 receptors with photolysis up to 90 ms after electrical stimulation. The amplitude of the IPSC was not affected with photoactivation of CyHQ-sulpiride at times later than 90 ms. Thus, the functional interaction between dopamine and the D2 receptor occurred at spatially defined spots of dopamine release that preceded the peak of the IPSC. Together, the results reveal that the IPSC reaches a peak amplitude after localized spots of dopamine activate D2 autoreceptors for about 100 ms. This approach using CyHQ-sulpiride defines the period of dopamine/receptor interaction that is independent of the slower (by 10 times) downstream processes that underlie the IPSC and suggests the viability of generalizing these methods to other GPCR synapses.

## RESULTS AND DISCUSSION

The release of extracellular dopamine triggered by electrical stimuli was measured using the viral expression of dLight1.3b. Imaging was carried out using a 2-photon microscope with full field frame scans ( $20 \times 20 \mu\text{m}$ ) at a single z-plane (about  $1 \mu\text{m}$ ). With this approach widely isolated spots ( $1.5\text{--}3 \mu\text{m}$  in diameter) of fluorescence following electrical stimulation required extensive searching and were strikingly obvious once encountered (Figure 1). The density of release sites found in the substantia nigra was distinctly lower than that found in the striatum. This was expected since the amount of release in the striatum measured with voltammetry is close to 1,000 times greater than in the substantia nigra (Ford et al., 2010). Thus, although the density of release sites observed with dLight in the substantia nigra was low and scattered the results suggest that the high concentration of dopamine that is required to mediate the D2-receptor-dependent IPSC is very localized. The fluorescence increase measured in the full field returned to baseline in about 2 frames and remained a low level (Figure 1). Treatment with cocaine ( $10 \mu\text{M}$ ) increased the duration of the fluorescence indicating that dopamine reuptake controlled the extent of diffusion in the midbrain (Figure S1).

The fluorescence in the distinct spots rose and fell in a single frame (200 ms, 5 Hz, Figure 1). To obtain the kinetics of the rise and fall of fluorescence in the isolated hotspots, line scans (2 ms/line) were carried out (Figure 1). The initial increase in fluorescence following stimulation peaked in 10 ms after a single stimulus ( $n = 4$ ) and 45 ms ( $n = 6$ ) following 2 stimuli (@ 40 Hz) and decayed with a time constant of 120 ms ( $n = 3$ , single stimulus) and  $182 \pm 44$  ms ( $n = 6$ , 2 stimuli, Figure 1). The rise and fall of extracellular dopamine

in the substantia nigra were similar to high concentration of dopamine found in spots of fluorescence reported in the striatum using dLight1.2 (Patriarchi et al., 2018).

Prior to probing of the interaction between endogenously released dopamine and D2 autoreceptors with CyHQ-sulpiride, the time course of D2 receptor blockade with photoactivation of CyHQ-sulpiride was examined using exogenous application of dopamine. Recordings were made from neurons in the substantia nigra and dopamine (10  $\mu$ M) was added to a recirculating solution containing CyHQ-sulpiride (15  $\mu$ M, recirculated for at least 5 min prior to use). Photolysis was accomplished with a full field flash of light through the objective (50 ms, 365 nm, 10 mW). Following photo-release of sulpiride, the outward current induced by dopamine was completely blocked with a time constant of  $228 \pm 28$  ms (mean  $\pm$  SD,  $n = 7$ , Figure 2). There was a small delay between the onset of light exposure and current suppression. Following the onset of the flash, the time it took to reach 5% of the total decline in current was  $106 \pm 17$  ms ( $n = 7$ , Figure 2). A visible deflection of current commenced by the end of the 50 ms flash. The delay in the onset of current decline is likely the combination of the off rate of dopamine from the receptor and the GTPase activity of Ga and the rebinding of G $\beta\gamma$  subunits.

Next, transient outward currents were induced with focal iontophoretic application of dopamine (20 nA, 5–20 ms). Photolysis of CyHQ-sulpiride to block the dopamine-induced current that was dependent on the relative timing of the iontophoretic pulse and the start of the 50 ms flash (Figure 2). Photolysis before the onset of the iontophoretic pulse completely blocked the outward current (data not shown). The time constant of the sulpiride-induced decay in the current induced by dopamine ( $223 \pm 43$  ms,  $n = 12$ ) was independent of the amplitude of the outward current (Figure 2). One striking observation was that the time it took to reach the peak outward current induced by the iontophoretically applied dopamine was dependent on the timing of the flash (Figure 2). As the timing of the flash approached the peak of the outward current, the latency to the onset of decline in the dopamine current decreased. There are two possible explanations for the change in latency. First there is a latency of about 50 ms between the application of dopamine and the initial rise in current, a rate inherent to the signal transduction. Second, at early time points photoactivation of sulpiride and dopamine compete for receptor occupation. At later times, the concentration of dopamine is falling such that the latency to current decline was dependent on dopamine leaving the receptor. In all cases, despite changes in the latency of decline, the time constant of the sulpiride induced current decay was the same. The results indicate that CyHQ-sulpiride can be used to determine the time course of interaction between dopamine and D2 receptors that mediate the IPSC.

Next, the inhibition of the IPSC induced by CyHQ-sulpiride was examined. As previously reported the kinetics of the dopamine-dependent IPSC in the substantia nigra scale with amplitude (Figure 2, supplement; Beckstead et al., 2004; Courtney and Ford, 2014). The IPSC had a latency of about 50 ms, peaked in  $275 \pm 28$  ms ( $n = 21$ , mean  $\pm$  SD), the duration measured at the half amplitude was  $403 \pm 86$  ms, and the time constant of decay that was  $355 \pm 82$  ms. Each of these measures did not consistently vary with increased stimulus intensity and current amplitude. The kinetics of IPSCs evoked by single, pairs (25

ms interval), and trains (5 @ 40 Hz) of electrical stimulation was examined. In each case, the time course of the IPSCs were unchanged with the intensity of the stimulus (Figure S2).

The IPSC was examined in experiments using systematic antagonism of the D2 receptors with photolysis of CyHQ-sulpiride before and following electrical stimulation. Initial experiments used a single electrical stimulus (1/min) to maximize temporal resolution. A solution of CyHQ-sulpiride (15  $\mu$ M) was recirculated for a period for at least 5 min. A single flash (50 ms, 10 mW) was sufficient to completely block the IPSC for at least 10 min, followed by partial recovery over about 30 min. Thus, each experimental replicate required a separate slice preparation. The timing of the flash was moved in steps ranging from 100 ms before the electrical stimulus to 500 ms after the stimulation. In each experiment, the effect of photolysis of CyHQ-sulpiride on the IPSC was compared with the previous IPSC as control. The amplitude of the IPSC induced in conjunction with photolysis was plotted relative to the preceding (control) IPSC (Figure 3).

The results show that photolysis of CyHQ-sulpiride before or simultaneous with the single electrical stimulus blocked the IPSC. Thus, receptors were blocked within ms following photolysis of CyHQ-sulpiride. As the time of photoactivation of sulpiride was moved to 30, 60, and 90 ms following the stimulus, the inhibition became partial such that amplitude of the IPSC increased (Figure 3). After 90 ms, the amplitude of the IPSC was almost unchanged by photolysis of the CyHQ-sulpiride. Thus, extracellular dopamine contributes to the peak of the IPSC for ~90 ms. Although the duration of the IPSC measured at 50% of the peak decreased following photoactivation of sulpiride at different time points, the time constant of current decay following the flash was the same across all experiments (Figure 3). In addition, the time it took to reach the peak current after photolysis was about 200 ms in experiments where the timing of the flash was less than 90 ms after the electrical stimulation. In experiments where photolysis was 90 ms or later, the time to reach the peak amplitude decreased (Figure 3). This observation is similar to that obtained using iontophoretic application of dopamine (Figure 2) with the exception that the kinetics of the synaptically released dopamine contributing to peak current was dramatically faster than exogenously applied dopamine. Taken together the results suggest that a high concentration (30–100  $\mu$ M, Ford et al., 2009) of synaptically released dopamine binds to the D2 autoreceptor in less than 30 ms to set in motion the downstream processes that activate the GIRK conductance. The consistency of flash-induced time-to-peak relative to the timing of the photolytic flash at the early stages of the IPSC suggests the concentration of dopamine must stay high in order to continue producing the same rate of rise in the IPSC. Though dopamine concentration is falling in this time frame, as seen both by dLight (Figure 1) or conceptual modeling (Cragg and Rice 2004; Wiencke et al., 2020), concentrations must still be high enough to almost maximally activate receptors during the time that defines the rising phase of the IPSC. This conclusion is also supported by experiments using excised macropatches of dopamine neurons where the duration of ligand-receptor interaction was found to determine the full amplitude of GIRK conductance (Ford et al., 2009; Courtney and Ford, 2014). The sulpiride induced block of receptors 30 and 60 ms following electrical stimulation decreased the amplitude of the IPSC but the initial rate of rise was the same as in control indicating that a high concentration of dopamine reached the receptors.

Pairs and trains of stimuli (2 or 5 at 40 Hz) were examined next. A flash 90 ms after a single stimulus decreased the IPSC to  $82\% \pm 3\%$  ( $n = 3$ ) of control but following a pair of stimuli or train of stimuli (5 @ 40 Hz) the IPSC was reduced to  $69\% \pm 15\%$  ( $n = 4$ ) and  $51\% \pm 13\%$  ( $n = 7$ ) of control ( $n = 4$ ), respectively. Photolysis 120 ms after the start of a train of stimuli reduced the IPSC amplitude to  $61\% \pm 18\%$  of control ( $n = 7$ ) and flashing at 240 ms was  $90\% \pm 7\%$  of control ( $n = 5$ ). The results suggest that dopamine release continues with each stimulus so that the timing of receptor blockade by sulpiride moves to later time points. This result is notable due to the fact that the duration of the IPSC is the same after 1, 2, and 5 stimuli (Figure S3).

The decline in potassium current induced by photolysis of CyHQ-sulpiride is more rapid than the decline of the IPSC. The time constant of decline in the IPSC was  $304 \pm 6$  ms ( $n = 78$ ), whereas the time constant decline in the IPSC following photolysis was  $253 \pm 6$  ms ( $n = 36$ ). Thus, the duration of the IPSC was greater than the termination of the IPSC induced by CyHQ-sulpiride even when photolysis was late enough to have no effect on peak amplitude (ANOVA,  $p < 0.001$ , Tukey post hoc). The decline in current induced by exogenous application of dopamine was  $220 \pm 41$  ms ( $n = 28$ ,  $p > 0.05$  ANOVA, Tukey post hoc). Thus, under normal circumstances the duration but not the peak of the IPSC is dependent on the continued presence of dopamine that could be the result of rebinding of dopamine or diffusion away from the release site.

One unexpected consequence of experiments using the CyHQ-sulpiride was a small ( $6.8 \pm 4.0$  pA,  $n = 21$ ) and reproducible inward current that decayed with a time constant of about 200 ms. This inward current was larger in experiments following the viral overexpression of D2 receptors or the application of cocaine ( $3 \mu\text{M}$ ,  $25.2 \pm 13.8$  pA,  $n = 12$ ). The inward current was only observed once in each slice, but was not observed following the superfusion of sulpiride or after treating the slice with reserpine to deplete vesicular dopamine (Rodriguez-Contreras et al., 2021). The results indicate that there was a very low level of D2-receptor activation and GIRK conductance resulting from tonic levels of extracellular dopamine.

The activation of the GIRK conductance mediated by GPCRs is dependent on both the concentration and the duration of agonist application. Short-duration applications (5–10 ms) of a saturating agonist concentration result in currents that peak in 100–300 ms. Longer applications (50–150 ms) result in larger amplitude currents with similar rise times (Sodickson and Bean, 1996; Ford et al., 2009; Courtney and Ford, 2014). The results of the present study indicate that synaptically released dopamine acts on the D2 autoreceptors for about 90 ms so that the IPSC reaches a peak in 200–300 ms (Figure 4). With continued release induced by trains of stimuli, the IPSC scales to that induced by a single stimulus (Figure S2), indicating, as observed with exogenous application of dopamine, that the duration of the current induced by receptor activation is dependent on downstream processes.

Given that the affinity of the  $G\beta\gamma$  subunits for GIRK is very low ( $100$  s of  $\mu\text{M}$ ) both the peak amplitude and duration of GIRK conductance is dependent on the sequestration rate of  $G\beta\gamma$  subunits by GDP-bound  $G\alpha$  subunits (Wang et al., 2016; Touhara and MacKinnon, 2018).

By increasing the duration of dopamine release using a train of stimuli for up to 125 ms (5 pulses at 40 Hz) more G $\beta\gamma$  subunits are liberated thus increasing the number of G $\beta\gamma$ -bound GIRK channels.

The decline could be determined by the affinity of dopamine for the receptor and/or GTPase activity of the G $\alpha$  subunits. Experiments with the photoactivation of sulpiride on the current induced by noradrenalin showed that the decline in current was more rapid than currents induced by dopamine (Figure S3). The suggestion is that the affinity of noradrenalin for the D2 autoreceptor is less than that of dopamine. Thus, the decline in the IPSC is at least in part dependent on the affinity of dopamine.

Taken together, the concentration of dopamine following dendritic release peaks and declines more rapidly than the activation of the GIRK-dependent IPSC (Ford et al., 2009). The rise to the peak of the IPSC is dependent on a concentration approximating 100  $\mu$ M for roughly 90 ms, 150 ms prior to the peak amplitude of the IPSC. The decay of the IPSC is somewhat longer than expected based on the block of receptors by photoactivated sulpiride. Thus, the time course of the IPSC is determined by both the GTPase activity of the G $\alpha$  subunits and the decline in the concentration of dopamine in the extracellular space. The late component of the IPSC is most likely the result of the trailing component (200–300 ms) of extracellular dopamine measured with dLight (Figure 4). Measures of the amplitude and kinetics of the IPSC were slowed in slices taken from animals that expressed dLight (Figure S4). This observation was taken as an indication that dLight buffered the released dopamine and increased the duration of the presence of dopamine as it dissociated from dLight.

That dopamine transmission is mediated by a synaptic or volume-dependent mechanism has been debated and modeled on multiple occasions (Cragg and Rice 2004; Wiencke et al., 2020). Dopamine-dependent transmission is clearly different from a truly synaptic mechanism. For example, glutamate is present in the synaptic cleft for less than 1 ms, and the time course of the NMDA-dependent transmission is dependent on the off rate of glutamate from the receptor ( $\tau = 250\text{--}400$  ms, Lester et al., 1990). Dopamine, on the other hand, must be present for about 100 ms to achieve the full amplitude of the IPSC. Given that the affinity of dLight1.3b for dopamine is roughly the same as the D2 receptors, the time course of the dLight transient correlates well with the functional experiments using the photoactivation of sulpiride. The dLight experiments also indicate that the concentration of dopamine (30–100  $\mu$ M) is present in highly localized spots for the required time (100 ms) to induce the IPSC. Thus, the diffusion of dopamine beyond the highly localized spots of release is not a major contributor to the amplitude of the IPSC.

## STAR★METHODS

### RESOURCE AVAILABILITY

**Lead contact**—Further information and requests for resources and reagents should be directed to and will be fulfilled by the lead contact, John Williams (williamsj@ohsu.edu)

**Materials availability**—This study did not generate new unique reagents.

### Data and code availability

- All data reported in this paper will be shared by the lead contact upon request.
- No new code was written for this study. All software used is publicly available and listed in the key resources table.
- Any additional information required to reanalyze the data reported in this paper is available from the lead contact upon request.

## EXPERIMENTAL MODEL AND SUBJECT DETAILS

The following mouse strain was used for this study: C57BL/6J – The Jackson Laboratories, Cat#: 000664. Male and female adult mice (100–150 days old) were used for all experiments. All procedures and experiments were approved by and done in accordance with the policies of the IACUC at Oregon Health & Science University and were bred and housed in an American Association for the Accreditation of Laboratory Animal Care (AAALAC)-accredited animal facility.

## METHOD DETAILS

**Slice preparation and electrophysiological recordings**—Mice were deeply anesthetized with isoflurane and decapitated. Brains were rapidly removed and slices (222  $\mu\text{M}$  thick) containing the substantia nigra were taken in the horizontal plane using a Leica vibratome and placed in a recovery chamber for > 30 minutes prior to experimentation. All preparation was done in warm (32 – 34°C) Krebs buffer containing (in mM) 126 NaCl, 1.2  $\text{MgCl}_2$ , 2.4  $\text{CaCl}_2$ , 1.4  $\text{NaH}_2\text{PO}_4$ , 25  $\text{NaHCO}_3$ , 11 D-glucose, along with 10  $\mu\text{M}$  MK-801 and continuous bubbling with 95%/5%  $\text{O}_2/\text{CO}_2$ . Following recovery, slices were placed in a recording chamber and perfused with Krebs buffer at a rate of 3 ml/min and maintained at 34 – 36°C. For all experiments NBQX 600 nM, picrotoxin 100  $\mu\text{M}$ , and CGP55845 300 nM were included in the solution to block AMPA, GABA-A, and GABA-B receptors. In all experiments, a gigaohm seal was made on a dopamine neuron in the substantia nigra with a glass electrode (1.3 – 1.8 megaohm resistance) filled with an internal solution containing (in mM) 10 BAPTA (4k), 90 K-methanesulphonate, 20 NaCl, 1.5  $\text{MgCl}_2$ , 10 HEPES (K), 2 ATP, 0.2 GTP, and 10 phosphocreatine. All cells were firing in a pacemaker fashion between 0.75 and 4 Hz and the firing frequencies were recorded. Then whole-cell voltage clamp recordings were made (hold at –55 mV). The cell capacitance, input resistance, and series resistance were documented.  $I_h$  currents were measured using a 60 mV hyperpolarization. D2-IPSC measurements were conducted in voltage clamp and continuously recorded and monitored using Chart 7 (AD Instruments, Colorado Springs, CO). Electrical stimulation with a bipolar metal stimulating electrode placed in the area of the substantia nigra was used to evoke D2 receptor dependent IPSCs. Stimulation with 1, 2 or 5 pulses (0.5 ms, 40 Hz) were used to evoke IPSCs (World Precision Instruments) once every minute and recorded with AxoGraph software (Berkeley, CA).

**Viral transduction**—Bilateral stereotaxic injections of AAV9 (Syn dLight1.3b, Vigene Biosciences) into the substantia nigra were done in mice anesthetized with isoflurane. The coordinates were AP –2.3 from bregma; ML  $\pm$  1.3; DV –4.5 mm. Injection volume was 120 nl. Experiments were done 1–3 weeks following the surgery.



**Pharmacology**—The application of drugs was done using bath superfusion in all experiments. CyHQ-sulpiride was kept as a stock solution in DMSO (30 mM) and diluted to a 15  $\mu$ M working solution. The working solution of CyHQ-sulpiride was recirculated in the bath (5 ml) for at least 5 min prior to photolysis. A ThorLabs M365LP1-C1 LED was used to photolyze CyHQ-sulpiride (5 mW, 365 nm, 50 ms). For all experiments NBQX 600 nM, picrotoxin 100  $\mu$ M, and CGP55845 300 nM were included in the solution to block AMPA, GABA-A, and GABA-B receptors. Dopamine iontophoresis was done using a thin-walled glass electrode (70–110 MW) with its tip placed within 40  $\mu$ m of the soma that was filled with 1 M dopamine, which was kept in place with a 4-nA backing current and ejected with a 10–50 ms, 25 nA pulse. Iontophoresis was controlled by an Axoclamp-2a amplifier with a 1X head stage. Dopamine (100 mM) was dissolved in water, kept at 4°C and diluted to 10  $\mu$ M in Krebs solution for superfusion. Forskolin was used to facilitate dopamine release specifically in experiments with the use of a single stimulus. This treatment increased the amplitude of the IPSC about 2-fold such that more accurate measurements of block by the CyHQ-sulpiride could be made. In previous publications forskolin have been shown to have little or no postsynaptic effect on the D2-receptor activation of potassium conductance. Given that the rate of current decay induced by CyHQ-sulpiride was the same for the IPSC and the exogenously applied dopamine, the results indicate that forskolin had no postsynaptic action on the kinetics.

**2-photon microscopy**—Imaging was carried out using a custom built 2-photon microscope with ScanImage software (Pologruto et al., 2003). Full frame images (128 $\times$ 128 pixels) were taken at a rate of 4 Hz. Line scans through areas of interest were taken at 2 ms/line.

## QUANTIFICATION AND STATISTICAL ANALYSIS

To analyze IPSC amplitudes, the maximum amplitude for a given IPSC was recorded between 200 and 400 ms following the stimulation onset. This range was used because the stereotyped peak of D2-IPSCs reliably falls within it and a measurement for very small or non-existent IPSCs would still be generated. Each reported value is the average of three consecutive stimulation events. Image analysis was done with Fiji: imageJ.

Statistical analysis was done using kaleidagraph. Student's t test was used for comparison of two groups while ANOVA was used to compare more than two groups or if there were multiple variables. Tukey's multiple comparison test was used if a repeated-measures ANOVA reached significance and Bonferroni post hoc comparisons were done if the one- or two-way ANOVA reached significance. Statistical details of experiments are found in the results section or figure legends for supplemental materials.

## Supplementary Material

Refer to Web version on PubMed Central for supplementary material.

## ACKNOWLEDGMENTS

This work was supported by the National Institutes of Health (R01 DA04523 to J.T.W., U01NS103522 to L.T., F31 DA047007 and K99 DA044287 to B.G.R.) and the Core Technology Platform resources at New York University Abu Dhabi (T.M.D.). We thank Drs. Kim Neve, Joseph Lebowitz, and Christopher Ford for insightful discussions.

## REFERENCES

- Asad N, McLain DE, Condon AF, Gore S, Hampton SE, Vijay S, Williams JT, and Dore TM (2020). Photoactivatable dopamine and sulpiride to explore the function of dopaminergic neurons and circuits. *ACS Chem. Neurosci* 11, 939–951. [PubMed: 32077679]
- Beckstead MJ, Grandy DK, Wickman K, and Williams JT (2004). Vesicular dopamine release elicits an inhibitory postsynaptic current in midbrain dopamine neurons. *Neuron* 42, 939–946. [PubMed: 15207238]
- Courtney NA, and Ford CP (2014). The timing of dopamine- and noradrenaline-mediated transmission reflects underlying differences in the extent of spillover and pooling. *J. Neurosci* 34, 7645–7656. [PubMed: 24872568]
- Cragg SJ, and Rice ME (2004). DANCING past the DAT at a DA synapse. *Trends Neurosci.* 27, 270–277. [PubMed: 15111009]
- Ford CP, Phillips PEM, and Williams JT (2009). The time course of dopamine transmission in the ventral tegmental area. *J. Neurosci* 29, 13344–13352. [PubMed: 19846722]
- Ford CP, Gantz SC, Phillips PEM, and Williams JT (2010). Control of extracellular dopamine at dendrite and axon terminals. *J. Neurosci* 30, 6975–6983. [PubMed: 20484639]
- Gantz SC, Bunzow JR, and Williams JT (2013). Spontaneous inhibitory synaptic currents mediated by a G protein-coupled receptor. *Neuron* 78, 807–812. [PubMed: 23764286]
- Groves PM, and Linder JC (1983). Dendro-dendritic synapses in substantia nigra: descriptions based on analysis of serial sections. *Exp. Brain Res* 49, 209–217. [PubMed: 6832258]
- Hajdu F, Hassler R, and Bak IJ (1973). Electron microscopic study of the substantia nigra and the strio-nigral projection in the rat. *Z. Zellforsch. Mikrosk. Anat* 146, 207–221. [PubMed: 4362205]
- Lacey MG, Mercuri NB, and North RA (1987). Dopamine acts on D2 receptors to increase potassium conductance in neurones of the rat substantia nigra zona compacta. *J. Physiol* 392, 397–416. [PubMed: 2451725]
- Lester RA, Clements JD, Westbrook GL, and Jahr CE (1990). Channel kinetics determine the time course of NMDA receptor-mediated synaptic currents. *Nature* 346, 565–567. [PubMed: 1974037]
- Patriarchi T, Cho JR, Merten K, Howe MW, Marley A, Xiong WH, Folk RW, Broussard GJ, Liang R, Jang MJ, et al. (2018). Ultrafast neuronal imaging of dopamine dynamics with designed genetically encoded sensors. *Science* 360, eaat442.
- Pologruto TA, Sabatini BL, and Svoboda K (2003). ScanImage: flexible software for operating laser scanning microscopes. *Biomed. Eng. Online* 2, 13. [PubMed: 12801419]
- Robinson BG, Cai X, Wang J, Bunzow JR, Williams JT, and Kaeser PS (2019). RIM is essential for stimulated but not spontaneous somatodendritic dopamine release in the midbrain. *eLife* 8, 47972.
- Rodriguez-Contreras D, Condon AF, Buck DC, Asad N, Dore TM, Verbeek DS, Tjijssen MAJ, Shinde U, Williams JT, and Neve KA (2021). A signaling-biased and constitutively active dopamine D2 receptor variant. *ACS Chem. Neurosci* 12, 1873–1884. [PubMed: 33974399]
- Schindelin J, Arganda-Carreras I, Frise E, Kaynig V, Longair M, Pietzsch T, Preibisch S, Rueden C, Saalfeld S, Schmid B, et al. (2012). Fiji: an open-source platform for biological-image analysis. *Nat. Methods* 9, 676–682. [PubMed: 22743772]
- Sodickson DL, and Bean BP (1996). GABAB receptor-activated inwardly rectifying potassium current in dissociated hippocampal CA3 neurons. *J. Neurosci* 16, 6374–6385. [PubMed: 8815916]
- Touhara KK, and MacKinnon R (2018). Molecular basis of signaling specificity between GIRK channels and GPCRs. *eLife* 7, e42908. [PubMed: 30526853]
- Wang W, Touhara KK, Weir K, Bean BP, and MacKinnon R (2016). Cooperative regulation by G proteins and Na(+) of neuronal GIRK2 K(+) channels. *eLife* 5, e15751. [PubMed: 27074662]

Wiencke K, Horstmann A, Mathar D, Villringer A, and Neumann J (2020). Dopamine release, diffusion and uptake: A computational model for synaptic and volume transmission. *PLoS Comput. Biol* 16, e1008410.

Wilson CJ, Groves PM, and Fifková E (1977). Monoaminergic synapses, including dendro-dendritic synapses in the rat substantia nigra. *Exp. Brain Res* 30, 161–174. [PubMed: 598426]

Author Manuscript

Author Manuscript

Author Manuscript

Author Manuscript

### Highlights

- Spatially discrete sited dopamine release is detected with the dopamine sensor dLight1.3b
- Kinetics of the rise and fall of extracellular dopamine is determined with dLight1.3b
- The dopamine/receptor interaction is determined using photoactivation of caged sulpiride
- The dopamine/receptor interaction is limited to about 100 ms following dendritic release

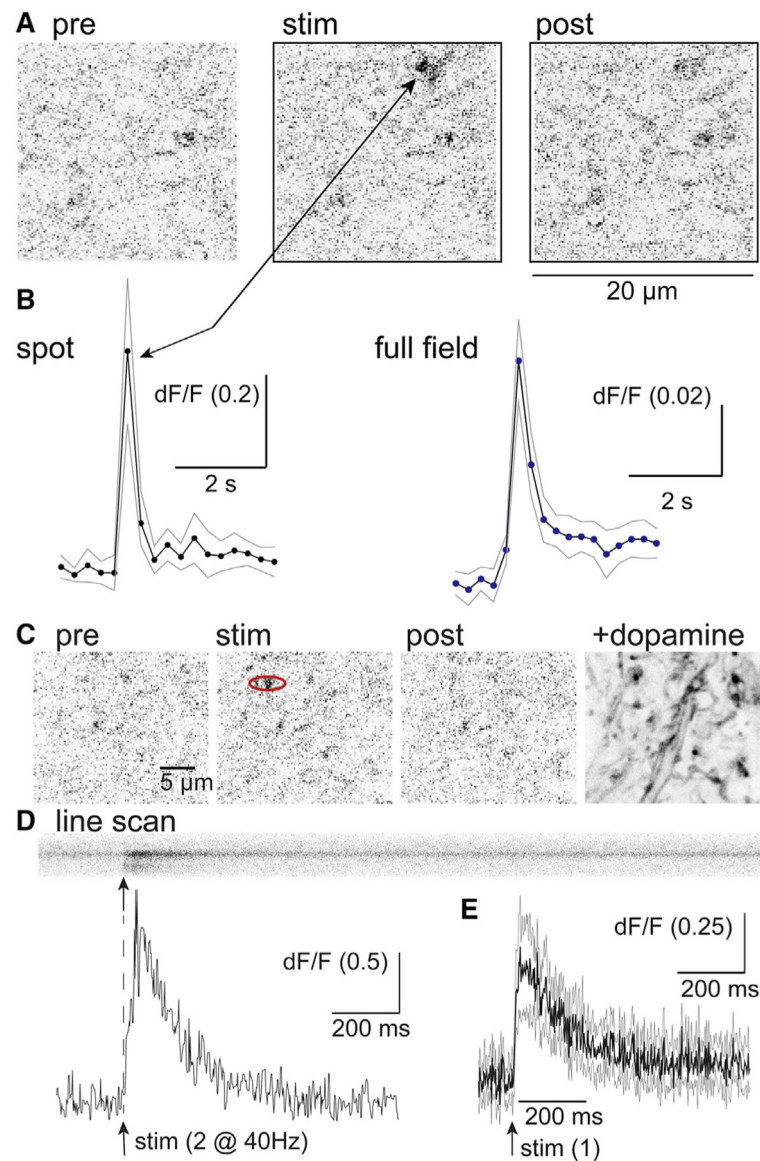


**Figure 1. Location and kinetics of dopamine release measured with dLight1.3b**

(A) Images of the activation of dLight upon electrical stimulation (frame rate 4 Hz). At frame 9 a pair of electrical stimuli were applied. Scale bar, 20  $\mu\text{m}$ .

(B) The fluorescence increase in a spot was measured in each frame and plotted below. The fluorescence for the entire frame (full field) is plotted on the right.

(C) Images of the activation of dLight upon electrical stimulation. A line scan was carried out along the spot in the red ellipse. Scale bar, 5  $\mu\text{m}$ .

(D) High temporal resolution measure of the rise and fall of dopamine measured with a line scan through a spot of dLight1.3b fluorescence. Below is the rise and fall of the fluorescence measured using the line scan above.

(E) Summary of the time course of dLight fluorescence obtained from line scans of 4 different spots (4 slices, 3 animals). The dark line is the mean change in fluorescence, and the gray lines are the 95% confidence limits.

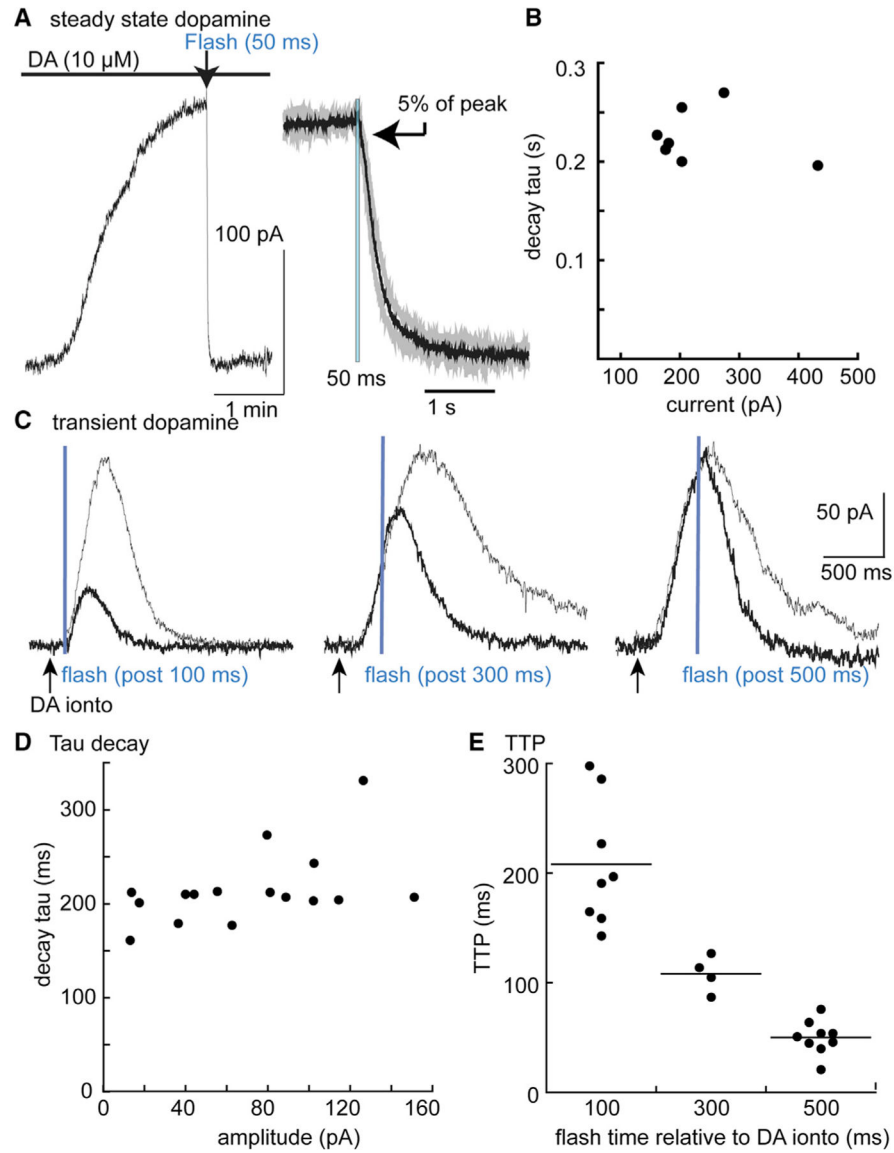


**Figure 2. Photolysis of CyHQ-sulpiride blocked D2-autoreceptor activation of GIRK**

(A) Left: an experiment where dopamine (10  $\mu$ M) was applied in the presence of CyHQ-sulpiride (15  $\mu$ M) and a flash (365 nm, 5 mW, 50 ms) was applied at the arrow. The right side is a summary of results (n = 7) where the current induced by sulpiride was normalized and averaged. The black line is the mean and the gray lines are the 95% confidence limits. The arrow indicated the point at which the current declined to 5% of the maximum ( $106 \pm 17$  ms following the onset of the 50 ms flash).

(B) Summary of experiments illustrating the time course of current block as a function of the amplitude of the current induced by dopamine (10  $\mu$ M).

(C) Traces showing individual experiments with a control current induced by iontophoretic application of dopamine (gray line) superimposed on the current induced by dopamine followed by photolysis of CyHQ-sulpiride (black line). The flash was applied at different times (100, 300, 500 ms) following the iontophoretic application of dopamine.

(D) Plot of the decay of the outward current induced by photolysis of CyHQ-sulpiride as a function of the amplitude of the outward current.

(E) Summarized results showing the time to reach the peak current relative to the onset of the flash.

Author Manuscript

Author Manuscript

Author Manuscript

Author Manuscript

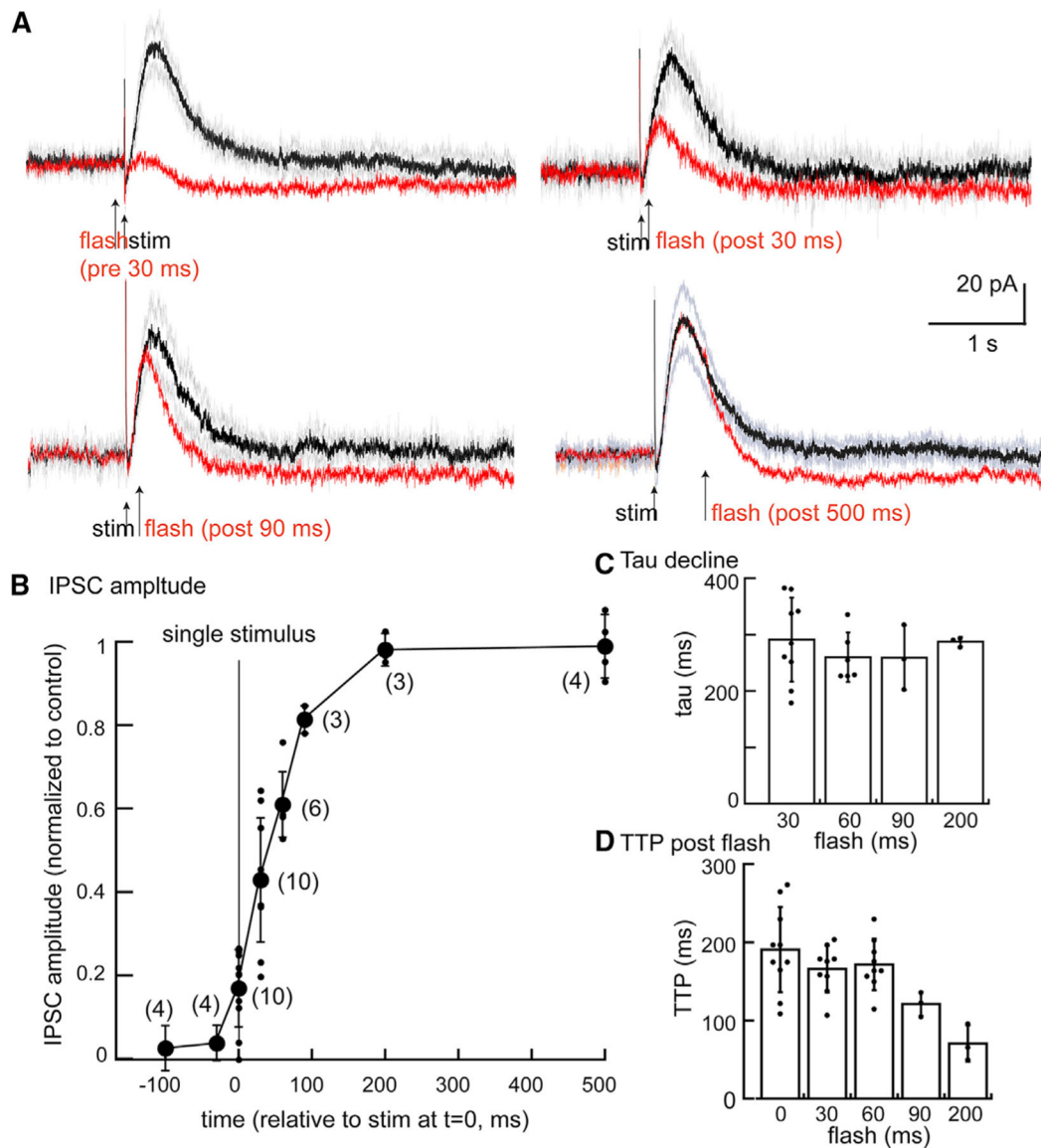


**Figure 3. Photolysis of CyHQ-sulpiride blocks the D2-autoreceptor IPSC in a graded manner dependent on the timing of the flash**

(A) Summary of experiments where photolysis was applied at 30 ms prior to the electrical stimulus, 30, 90, and 500 ms post stimulus. Each point is from a separate slice.

(B) Plot of the amplitude of the IPSC following photolysis relative to the prior (control) IPSC. The electrical stimulus was applied a 0 ms, and photolysis was induced at the indicated times on the x axis (mean  $\pm$  SD).

(C) Plot showing the time constant of decay following the flash was not dependent on the timing of the flash (mean  $\pm$  SD).

(D) Plot of the time it takes to reach the peak of the IPSC relative to the onset of the flash (mean  $\pm$  SD).



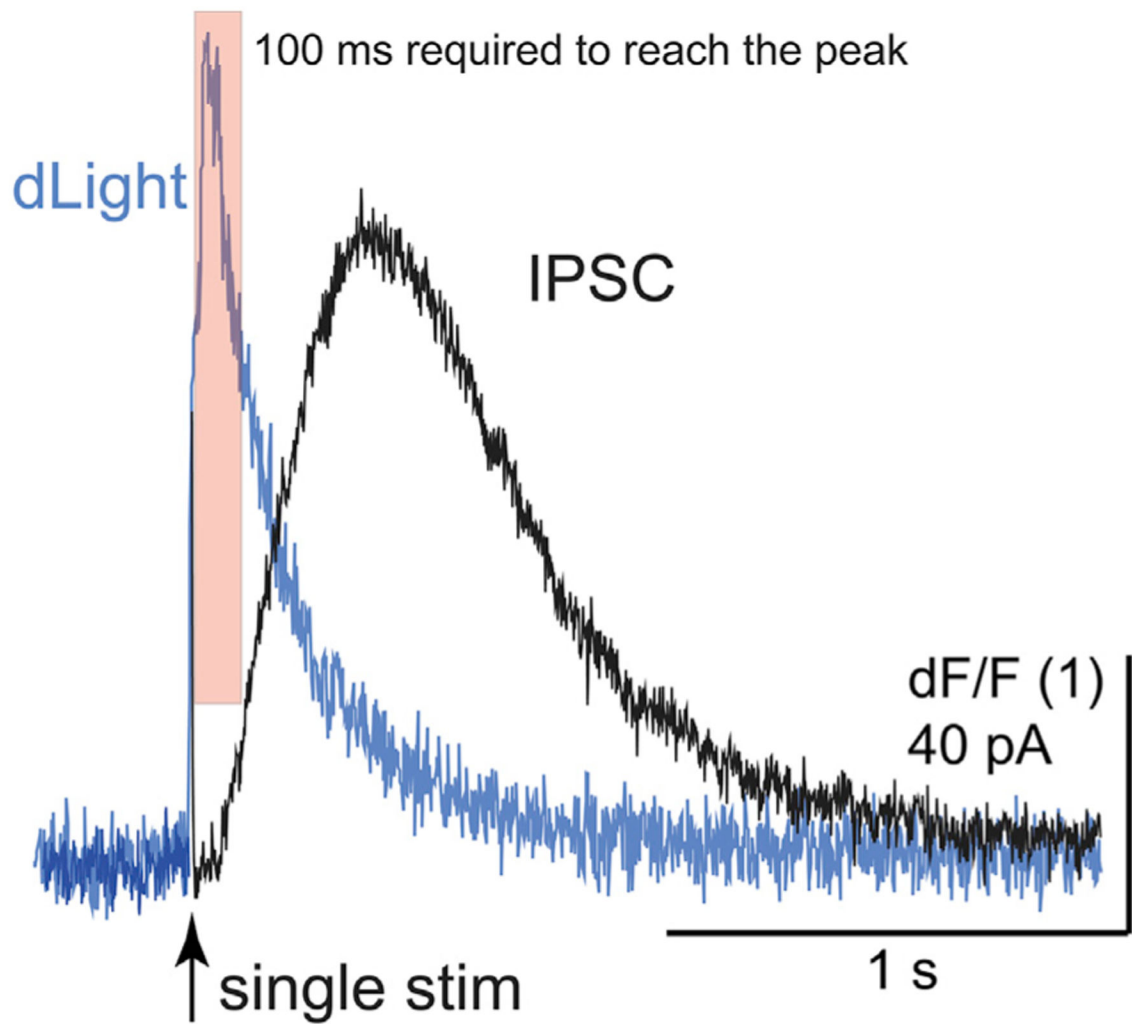


**Figure 4. Illustration of the relative time course of the rise and fall of extracellular dopamine measured with dLight superimposed on the IPSC**  
 This illustration is taken from two different experiments (dLight imaging, IPSC recording). The shaded red box indicates the 90 ms where most of the amplitude of the IPSC is induced. The remainder of the fall in extracellular dopamine is suggested to result in prolongation of the IPSC.

## KEY RESOURCES TABLE

REAGENT or RESOURCE	Source	IDENTIFIER
Bacterial and virus strains		
AAV9	Vigene Biosciences	N/A
Chemicals, peptides, and recombinant proteins		
(+)-MK-801 nakeate	Hello Bio	Cat#HB0004
Forskolin	Hello Bio	Cat#HB1348
CGP55845 hydrochloride	Hello Bio	Cat#HB0960
NBQX	Hello Bio	Cat#HB0442
CyHQ-sulpiride	Asad et al., 2020	N/A
Experimental models: Organisms/strains		
C57BL/6J mice	The Jackson Laboratories	000664
Recombinant DNA		
pAAV-syn-DLight1.3b	Patriarchi et al., 2018	Addgene Cat#135762
Software and algorithms		
LabChart 7	AD Instruments, Colorado Springs, CO	N/A
AxoGraph	Berkley, CA	N/A
Fiji: ImageJ	Schindelin et al., 2012	N/A
KaleidaGraph	Synergy Software	N/A
ScanImage	Pologruto et al., 2003	N/A